

# **Estimation of whole-body averaged SAR of grounded human models for plane wave exposure at respective resonance frequencies**

Akimasa Hirata<sup>1</sup>, Kazuya Yanase<sup>1</sup>, Ilkka Laakso<sup>1</sup>, Kwok Hung Chan<sup>1</sup>, Osamu Fujiwara<sup>1</sup>, Tomoaki Nagaoka<sup>2</sup>, Soichi Watanabe<sup>2</sup>, Emmanuelle Conil<sup>3</sup>, and Joe Wiart<sup>3</sup>

1: Nagoya Institute of Technology, Department of Computer Science and Engineering, Japan

2: National Institute of Information and Communications Technology, Electromagnetic Compatibility Laboratory, Japan

3: Orange Laboratories, France

Corresponding Author: Akimasa Hirata

Address: Nagoya Institute of Technology, Gokiso-cho, Showa-ku, Nagoya 466-8555, Japan

Tel&Fax: +81-52-735-7916

E-mail: [ahirata@nitech.ac.jp](mailto:ahirata@nitech.ac.jp)

## **Abstract**

According to the international guidelines, the whole-body average specific absorption rate (WBA-SAR) is used as a metric of basic restriction for radio frequency whole-body exposure. It is well known that the WBA-SAR largely depends on the frequency of the incident wave for a given incident power density. The frequency at which the WBA-SAR becomes maximal is called the “resonance frequency.” Our previous study proposed a scheme for estimating the WBA-SAR at this resonance frequency based on an analogy between the power absorption characteristic of human models in free space and that of a dipole antenna. However, a scheme for estimating the WBA-SAR in a grounded human has not been discussed sufficiently, even though the WBA-SAR in a grounded human is larger than that in an ungrounded human. In the present study, with the use of the finite-difference time-domain method, the grounded condition is confirmed to be the worst-case exposure for human body models in standing posture. Then, WBA-SARs in grounded human models are calculated at their respective resonant frequencies. A formula for estimating the WBA-SAR of a human standing on the ground is proposed based on an analogy with a quarter-wavelength monopole antenna. First, homogenized human body models are shown to provide conservative WBA-SAR as compared with anatomically-based models. Based on the formula proposed here, the WBA-SARs in grounded human models are approximately 10% larger than those in free space. The variability of WBA-SAR was shown to be  $\pm 30\%$  even for humans at the same age, which is caused by the body shape.

## 1. Introduction

There has been concern about the adverse health effects of human exposure to electromagnetic (EM) waves and thus the world health organization issued the research agenda for radio-frequency fields (WHO 2010). Based on the international guidelines/standards (ICNIRP 1998, IEEE 2006), the whole-body average specific absorption rate (WBA-SAR) is used as a metric of basic restriction for whole-body exposure at radio frequencies. The limit is 0.4 W/kg for occupational exposure or 0.08 W/kg for the general public (ICNIRP 1998, IEEE 2006).

It is well known that the WBA-SAR largely depends on the frequency of the incident wave even at the same incident power density. For human models exposed to vertically-polarized plane waves in free space, the WBA-SAR has a clear peak at several dozen megahertz in adults (Dimbylow 2002, Dimbylow 2005, Hirata *et al* 2007, Conil *et al* 2008, Dimbylow *et al* 2008, Hirata *et al* 2010) and at one hundred and a few tens of megahertz in children (Dimbylow and Bolch 2007, Conil *et al* 2008, Nagaoka *et al* 2008, Hirata *et al* 2010). This peak is attributed to a standing wave along the human height direction. In this research field, the frequency at which the WBA-SAR becomes maximal is called the “resonance frequency.” At the resonance frequency, the human height is approximately 0.4 times the wavelength in free space. This relationship between human height and the wavelength at the free-space resonance frequency was originally derived from a highly simplified prolate spheroid or homogeneous block models (Durney 1980, Gandhi 1980), and then confirmed using anatomically realistic models in recent studies (Dimbylow 1997, Dimbylow 2002, Dimbylow 2005, Hirata *et al* 2010).

For humans standing on a perfectly conducting ground plane, the resonance frequency is almost half that for humans in free space. In addition, the WBA-SARs of the grounded ellipsoids at their resonance frequencies were larger than those in free space (Gandhi 1980). For separations from ground of more than 7–10 cm, the WBA-SAR and SAR distribution are considered as almost identical to those in free space (Gandhi 1980). No study, however, investigated the dependence of WBA-SAR on the model-ground separation. Furthermore, only two research group investigated WBA-SARs in the grounded condition of anatomically based human models (Dimbylow 1997, Dimbylow 2002, Dimbylow 2005, Findlay and Dimbylow 2008, Lee and Choi 2012). Thus, the variability of WBA-SARs in different grounded human body models, including realistic children and pregnant women, is also of interest. Note that it is difficult to develop different experimental and numeric human models due to significant time and cost requirements (Kawamura *et al* 2010). Thus, it is desirable to develop a scheme to estimate WBA-SARs for humans in grounded condition.

In the present study, we first discuss our investigation of the dependence of WBA-SARs on the human-ground distance in order to confirm the worst-case exposure condition. Then, we present an intercomparison of WBA-SAR values in order to confirm our computational results.

Furthermore, a formula for estimating the WBA-SAR of grounded human models is proposed based on an analogy to a quarter-wave monopole antenna. Finally, the variability of the WBA-SAR in humans with different ages and body shapes is estimated based on the proposed formula.

## **2. Model and Methods**

### **2.1. Human Body Models**

Thirteen human body models were considered, including the Japanese male and female models named TARO and HANAKO, respectively, (Nagaoka *et al* 2004) and three-, five-, and seven-year-old child models developed from TARO (Nagaoka *et al* 2008). TARO and HANAKO models are segmented into 51 tissue types. A pregnant woman model with a gestation period of 26 weeks was also considered, taking into account 56 anatomic tissue types (Nagaoka *et al* 2007).

In addition, an European male model named Duke; a female model named Ella; an eleven year-old female child, Billie; and a six year-old male child, Thelonious, were also used (Christ *et al*, 2010). These models comprise 84 tissues. Two other well-characterized European male and female models, named NORMAN and NAOMI and consisting of 37 and 41 tissue types, were also included (Dimbylow 1997, 2005). Furthermore, a model developed at Brooks Air Force Base (BAFB) was also used. In this study, the resolution of each model is 2 mm. The height, weight, body mass index (BMI), and the number of tissue types for these models are summarized in table 1. As investigated later, the variability of WBA-SAR is estimated using empirical estimation. According to the reference human defined in the International Commission on Radiation Protection, the average height and weight of the adult male are 174.5 cm  $\pm$ 6.6 cm and 71.7 kg  $\pm$ 10kg, while 162.6 cm  $\pm$ 6.6 cm and 56.7 kg  $\pm$ 8.6 kg for the adult female (ICRP 1975).

### **2.2. Computational Methods**

The finite-difference time-domain (FDTD) method was used to calculate the electromagnetic power absorbed in the human models. The FDTD method is most commonly used in the RF dosimetry for its capability to handle lossy dielectric medium like human body. The FDTD grid is discretized at 2 mm so as to coincide with the resolution of the human models. For geometries in which the wave-object interaction has to be considered in open regions, the computational space has to be truncated by absorbing boundaries. We use perfectly matched layers (PML) consisting of 12 layers as the absorbing boundaries. The distance between the model surface and absorbing boundary was set as 30 cells. Note that the separation of the body model from PML marginally affects the SAR; the maximum percentage difference in SAR values was reported as

1.8% when the number of cells between body and PML is increased from 2 and 70 for frequencies above 70 MHz under the plane wave exposure in free space (Findlay and Dimbylow 2006). The same tendency was confirmed by Laakso *et al* (2007). In addition, the same tendency was confirmed for the code developed at the Nagoya Institute of Technology. For modeling grounded condition, the human model is assumed to be standing on an infinite perfectly conducting ground plane.

The electrical properties of tissues have been determined from the four Cole–Cole model by Gabriel *et al* (1996). The electrical properties of tissue types that were not described in Gabriel *et al* (1996) have been substituted for those of similar tissues. The electrical properties of the child were assumed to be identical those of the adults. Note that the age dependencies of measured dielectric constants have been reported for animals (Peyman *et al* 2009). In that study, the primary factor affecting the dielectric constants is the water content of tissues. Our assumption is supported by the facts that 1) the dielectric properties of tissues are mainly determined by their water content (Peyman *et al* 2009) and 2) the difference of the total body water content between a 3-year-old child and a 22-year-old adult is less than 10% (Altman and Dittmer 1974), which leads to a difference of a few percent or less in the dielectric constants of the human body (Wang *et al* 2006).

When considering homogeneous human models, the electrical constants were taken to be  $2/3$  that of muscle. Note that the human body is comprised of high- and low-water-content tissues in the ratio of 2:1. The electrical constants of low-water-content tissues, such as fat and bone, are much smaller than those of high-water-content tissues, such as muscle. Therefore, an electrical constant of  $2/3$  that of muscle, which is representative of high-water-content tissue, is often assumed for fundamental discussions.

### **2.3. Exposure Scenarios**

One of the models is chosen and assumed to be standing on the ground (see figure 1). As an incident wave, a plane wave with a vertical polarization is considered. The plane wave is incident on the human models from the front (along the anteroposterior direction). The reason for choosing this incident direction is that it results in a higher WBA-SAR compared to incident directions directly and obliquely from the above (Findlay and Dimbylow 2008). In addition, in free space, the incident angle in the horizontal plane has minor effect on the WBA-SAR at frequencies lower than 300 MHz (Nagaoka *et al* 2008, Kühn *et al* 2009, Uusitupa *et al* 2010); the same is likely to be true also in grounded conditions. Different human-ground distances were considered in order to verify that the WBA-SAR in the grounded human is maximal. The WBA-SARs in models of different postures, e.g., with the arms vertically upwards, have been reported to be larger than in those standing up straight (Findlay and Dimbylow 2005, Uusitupa

*et al* 2010). However, the effect of different postures on the WBA-SARs is not of concern in this study.

### **3. Computational Results**

#### **3.1. Verification of Computational Results**

In order to verify the computational results, the total absorbed power of the mother and fetus in the grounded Japanese pregnant woman model were calculated through independent efforts by researchers at three different institutes. The primary purpose of this section is to confirm that our computational code provide reasonable computational results. All the three institutes used their own in-house FDTD codes. Note that the FDTD method is the only method which can conduct the dosimetry for the human body model with a resolution of a few millimeters. Unlike Dimbylow *et al* (2008), we considered an exposure scenario of grounded condition, and also paid attention to the average power absorbed in the fetus, which is located in the internal part of the body. The incident power density was  $2 \text{ W m}^{-2}$ . The electromagnetic wave was incident from the front of the model. The frequency was 46 MHz, which is the resonance frequency for the grounded exposure condition. All the conditions were set to be identical. As seen from table 2, the values for the average power absorbed in the mother computed by all three groups are in good agreement. The difference between the highest and lowest estimates for the total absorbed power was 2.5% for the mother and 5.4% for the fetus. The former difference is in line with that reported in a previous intercomparison (Dimbylow *et al* 2008). The difference in the total power absorbed in the fetus was still small but larger than that observed in the mother. Note that the absolute value of the power absorbed in the fetus is much smaller than that of the mother. In the following, the results computed with the code developed at the Nagoya Institute of Technology will be presented.

Let us comment on the computational uncertainty in the computational results, which can be primarily classified into two factors. The first factor is, as mentioned in Sec. 2.2, the absorbing boundary condition. In our study the distance between the body model surface and the PML boundary (body-PML) was set as 30 cells. When changing the body-PML separation from 5 to 100 cells, the deviation of total power absorption in the human body was 2.4% or less when comparing the value at 30 cells. The second factor is the discretization of the grid. The frequency considered herein is from a few dozen megahertz to one hundred megahertz, and thus the discretization at 2 mm is fine enough as compared with the wavelength. Even though the model resolution of 4 mm is used, the computational error has been reported as  $\pm 1.2\%$  (Dimbylow 2002). Our computational uncertainty attributable to the grid discretization is expected to be smaller than that by Dimbylow (2002) and thus not investigated herein.

### 3.2. Dependence of WBA-SARs on Human Body-Ground Distances

Figure 2 shows the WBA-SAR in TARO for different human-ground distances at the grounded resonance frequency of 39 MHz. As shown in figure 2, the WBA-SAR decreases with increasing the human-ground distance. The primary reason for this decrease is the change of the resonance frequency for different human-ground distances. For separations from ground more than 70–100 mm, the WBA-SAR and SAR distribution in a homogeneous ellipsoid was considered as almost identical to those in free space (Gandhi 1980). For the human-ground distance of 100 mm, however, the difference of WBA-SARs of TARO in grounded condition and free space was 42%.

The resonance frequencies and the respective WBA-SARs were determined for different distances in the models of Japanese adult male and children. Figures 3(a) and (b) show the normalized WBA-SAR and the normalized resonance frequency, respectively, as a function of the relative distance (normalized by the respective model height) to the ground. Both the WBA-SAR and the resonance frequency have been normalized with respect to the free-space condition. As seen from figure 3(a), the normalized WBA-SARs oscillate with increasing distance and then seem to converge to unity (free space). Figure 3(b) shows that the resonance frequency increases rapidly when the human-ground distance increases from 0 to 20% of the model's height, after which the resonance frequency stays within 10% of that of free space resonance frequency. As shown in figure 3(a), the WBA-SAR is maximal in the grounded condition. Therefore, in the following discussion, the human models are assumed to be grounded.

### 3.3. Derivation of Formula for WBA-SAR Estimation Based on Analogy of Grounded Human Body and Monopole Antenna

In order to confirm the analogy between a monopole antenna and grounded human body models at their respective resonance frequencies, the conduction currents along the vertical axis were calculated for the Japanese models. As shown in figure 4, the amplitude of the conduction current crossing the horizontal plane of the human model resembles that for the monopole antenna. Several ripples, however, were observed in the conduction current distribution. These ripples appear because the effect of the displacement current is not negligible at or above approximately 10 MHz (Hirata *et al* 2001). Based on this similarity, the power absorbed in the human body is expected to be smaller than that of a monopole antenna with a matched load, because the human body does not act as a good conductor in this frequency region.

Let us summarize the fundamental characteristics of the monopole antenna, which is almost identical to that of the dipole antenna reviewed in Hirata *et al* (2010). For a current distribution on the antenna  $I(z)$  and a maximum current  $I_0$  [A], the effective height of the antenna  $L_e$  [m] is

given by the following equation (Kraus and Marhefka 2002):

$$L_e = \frac{1}{I_0} \int_0^L I(z) dz \quad (1)$$

where  $L$  [m] is the physical height of the antenna. The effective height of the monopole antenna is given by the following equation:

$$L_e = \frac{\lambda}{\pi} \cong 0.636L. \quad (2)$$

For an antenna of known effective height, the induced voltage  $V_o$  [V] can be approximated by multiplying the effective height by the incident electric field (a scaled square root of the incident power density  $S_{inc}$  [W/m<sup>2</sup>]):

$$V_o = \sqrt{120\pi S_{inc}} L_e \quad (3)$$

where  $120\pi$  [ $\Omega$ ] is the impedance of free space. From (2) and (3), we can estimate the induced voltage in the antenna.

Let's apply the above fundamental characteristics to the human body. Figure 5 (a) shows the relationship between the effective antenna height and the height of human body model for all the thirteen models listed in table 1. As shown in this figure, strong correlation was observed between the human height  $h$  [m] and the human effective height as an antenna  $h_e$  [m]. In the results for the Japanese models, the regression line obtained using the least squares method was represented as:

$$h_e = 0.782h \quad (4)$$

where the coefficient of determination was 0.982. From (2) and (3), the current distribution on the human body can be confirmed to be similar to a monopole antenna.

Next, the relationship between the approximate induced voltage  $V_o$  [V], determined from the effective height by (3), and the power absorbed in the human body was investigated in order to examine the radiation resistance considering the human body as an equivalent antenna. As seen from figure 5 (b), strong correlation was observed between the induced voltage and the total absorbed power  $P$  [W]. Their relationship is characterized by the least squares method using the following equation:

$$P = 3.45 \times 10^{-3} V_o^2. \quad (5)$$

The coefficient of determination was 0.940. From the reciprocal of the coefficient in (5), the radiation resistance for the human body was approximately constant at 292  $\Omega$ , even though the resonance frequency and body shape differ for different models. From (3), (4), and (5), we can obtain an equation to estimate the total power absorbed in the human. Then, the WBA-SAR in a human body model by the following equation:

$$\text{WBA-SAR} = P / W = 0.794 S_{inc} \cdot h^2 / W \quad (6)$$

where  $W$  is the weight of the human. The coefficient of determination was 0.859.

In order to discuss the effectiveness of the formula (6), the WBA-SARs in the anatomically based models calculated by the FDTD method and estimated from (6) are listed in Table 3. The incident power density is  $2 \text{ W m}^{-2}$ . As shown in the table, all of these values for Japanese models are within 10% of the average. (6) provides reasonable WBA-SARs even for different models; the maximal and average differences were 20.4% and 8.2%, respectively. Note that WBA-SARs in the child models were changed by less than 1% when using the dielectric constants derived from Wang *et al* (2006). Thus, the effect of the dielectric constants of tissue on the coefficient on (6) is marginal.

### **3.4. Effect of Model Inhomogeneity on WBA-SAR**

A conservative estimation of WBA-SARs is also of interest when discussing the relationship between the reference level and basic restriction in the guidelines/standard (ICNIRP 1998, IEEE 2005). As mentioned in the previous subsection, the formula (6) does not always provide a conservative estimate and thus may not be applicable to the above purpose. In order to clarify the reason for underestimation in some anatomical models by 10% or more, we investigated the conduction current distribution in a set of selected Japanese models and their homogenized models. As shown in figure 6, the conduction current at the ankle becomes smaller in inhomogeneous models than in those of homogenized models. The primary reason for this difference would be attributed to the model inhomogeneity. The dominant tissue in the cross section, including the ankle, is the bone, for which the conductivity is low (Gabriel *et al* 1996), resulting in a smaller conduction current. The same tendency was observed for different models not shown here.

Figure 7 shows the comparison of the WBA-SARs for homogeneous and inhomogeneous Japanese models. As seen from figure 7, the WBA-SARs in the homogenized model are larger than those of inhomogeneous models. The same tendency was observed even for different seven models, although not shown here to avoid repetition. One of the primary reasons for this is thought to be smaller current around the ankle due to the above-mentioned reason. When deriving the estimation equation for the homogeneous model, the coefficient of the estimation was 0.991 in (6), which was 24.8% larger than that of the inhomogeneous model. The formula with this coefficient should provide conservative WBA-SARs, which will be discussed in Sec. 3.5.

### **3.5. Variability of whole-body averaged SAR at the resonance frequency**

The variability of the WBA-SAR in different human models is discussed based on sections 3.3 and 3.4, as is similar to Hirata *et al* (2010), in which WBA-SAR in free space was discussed. As

is evident from (6), the WBA-SAR depends on the BMI only for the same incident power density. For statistical data of BMI for Japanese (Japanese Society for Pediatric Endocrinology 2011, Japanese Society of Nutritional Assessment for Japanese adult 2001), the variability of WBA-SAR due to the body shape is estimated. Note that in these references, the age dependency of BMI is listed in addition to the variability of height and weight of the body unlike ICRP (1975). Figure 8 illustrates the WBA-SAR for Japanese with BMI of 2.5–97.5%ile. In the same figure, estimated WBA-SAR for the inhomogeneous model with BMI of 2.5% to 97.5 ile, and that for homogeneous model with BMI of 2.5 %ile are plotted using equation (6). As seen from figure 8, the maximum WBA-SAR was observed in the normalized (50%ile) child of 5-7 years old because of their smallest BMI. The variability of WBA-SAR is estimated as  $\pm 20\text{-}30\%$  even for humans of the same age.

#### 4. Discussion

In a previous study (Gandhi 1980), the WBA-SAR and SAR distribution in an ellipsoid was considered as almost identical to those in free space. For the human-ground distance of 100 mm, however, the difference of WBA-SARs of TARO in free space was several dozen percent, suggesting that the position of ground may not be neglected even for longer distance than expected. Then, the WBA-SAR in a grounded human was confirmed to be highest by changing the distance between the human body and the ground.

Let us discuss the difference between the WBA-SARs of humans standing in free space and those that are grounded. Grounded human body models were considered approximately as monopole antennas. The human body models in free space were considered as dipole antennas (Hirata *et al* 2010). The radiation resistances of the monopole and dipole antennas are  $52\ \Omega$  and  $73.2\ \Omega$ , respectively. The open voltages of monopole and dipole antennas are identical from Eq. (2) as their effective heights are almost identical, although some difference could be observed when applying to the human body models (see also Hirata *et al* 2010). Then, the received power of the monopole antenna is 40.7% larger than that of the dipole antenna. Thus, the WBA-SAR of the grounded models should be 40.7% larger than those in free space. This tendency was expected from Gandhi (1980) in which homogeneous and simple-shaped models were considered. From Sec. 3.4, the coefficient characterizing the WBA-SAR for grounded homogeneous human models was 0.991, which is 33.7% larger than that for those in free space, 0.741 (Hirata *et al* 2010). This difference was somewhat smaller than the difference between monopole and dipole antennas. This difference supports the finding by Gandhi (1980) that the WBA-SARs for grounded humans are larger than those in free space. However, the coefficient characterizing the WBA-SAR for grounded anatomical human models was 0.794, which was only 5.8% larger than that for those in free space (Hirata *et al* 2010). This smaller difference

would be caused by smaller ankle current in anatomical models. The smaller ankle current in grounded models is caused by the smaller conductivities in that cross section including bone and fat.

In order to provide conservative WBA-SAR values for contributing the safety guidelines, we clarified that the WBA-SARs in the homogenized models are larger than those of the inhomogeneous model. The main reasons for this conservative estimation were attributed to the differences in the ankle current, in addition to the dielectric properties of the lower part of the human body. We substituted Japanese BMI into (6) to estimate the variability of WBA-SAR based on Japanese population covering 95%. The variability of WBA-SARs is primarily attributable to the BMI that can be characterized by the height and weight of the body. The point to be stressed here is that, in general, WBA-SAR may become maximal for the normalized child, which usually has a lower BMI than the normalized adult, as shown in Figure 8. The largest estimated WBA-SAR by equation (6) for humans with 2.5%ile at 3-7 years old was 0.12 W/kg, which is 50% larger than the basic restriction. Note that the value of WBA-SAR in children according to the calculation method stated in the ICNIRP guidelines may be 40% larger than that of the basic restriction for worst-case exposures (ICNIRP statement 2009). Note that the effect of anatomical composition on WBA-SAR is empirically discussed in Appendix, and shown to be marginal.

## **5. Summary**

This study calculated the WBA-SARs in grounded human models at their respective resonance frequencies by the FDTD method. First, our computational code was validated via intercomparison. Then, by computing the WBA-SAR for different distances between the human body and the ground plane, it was shown that the grounded condition results in the worst-case exposure for human body models in standing posture. From our computational results for 13 human voxel models, computation using the anatomically-based models suggests that the difference of WBA-SAR in free space and grounded was 5.8% (average), which is much smaller than that expected from an ellipsoidal mode of 20-30% (Gandhi 1980) and that derived from the antenna theory of 40.7%. Then, a formula for estimating the WBA-SAR was proposed based on an analogy with a quarter-wavelength monopole antenna. This formula estimates the WBA-SAR in terms of the height and weight of the human models only, with an uncertainty of a few dozen percent. In order to provide conservative WBA-SAR values which may be useful for setting the limit in the safety guidelines, we clarified that the WBA-SARs in the homogenized models are larger than those in the inhomogeneous models. The reason for this conservative estimation was attributed to the difference in the ankle current. In particular, the

WBA-SAR in children with lower BMI was suggested to become large. The development of such child models and WBA-SAR computation in the models would remain as future work.

### **Acknowledgements**

This research was supported in part by Strategic International Cooperative Program (Joint Research Type), Japan Science and Technology Agency and the France National Research Agency, and grant-in-aid for young scientist (B) from Japan Society for the Promotion of Science.

## Appendix A. Effect of Body Fat Percentage on WBA-SAR

One of the findings was that the total power absorption in the human can be estimated with the human height only (see Eq. (6)). Thus, the effect of model inhomogeneity is not taken into account. In our previous study (Hirata *et al* 2010), we discussed the WBA-SAR of the human models in free space and then proposed to take into account the body fat percentage (BFP) as a macroscopic index of model inhomogeneity. Note that the feature of BFP is easily measured/estimated like the human body height and weight (e.g., Lean *et al* 1996). Similar attempt has been conducted for the exposure scenario considered here.

Figure A.1 shows the effect of BFP on the WBA-SAR of different models, together with the results for a homogeneous Japanese adult male model comprised of  $\alpha\%$  muscle. All WBA-SARs in the anatomically based models were normalized by those of the corresponding homogenized models to  $2/3$  that of muscle. In addition,  $\alpha\%$  muscle is defined to have the electrical constants of muscle multiplied by  $\alpha\%$ , which is similar to  $2/3$  muscle. In other words,  $\alpha$  is a factor used to scale the dielectric property of the homogeneous model. As shown in figure 8, the WBA-SARs in the model are comprised of  $\alpha\%$  muscle, and the anatomically based models become smaller with increasing BFP. In order to extrapolate from the available data, regression lines approximated as a second-order polynomial are derived. The fundamental equation is as follows; the coefficient is revised based on the results for homogenized model and the compensation coefficient  $F$  is introduced.

$$WBASAR = 0.991F(p)S_{inc}h^2 / W \quad (A1)$$

$$F(p) = -5.0 \times 10^{-5} p^2 - 0.0055 p + 0.99 \quad (A2)$$

where  $p$  is the BFP. From (A2), the uncertainty due to the BFP can be roughly estimated. This figure suggests that the model homogenized with  $2/3$ -muscle would provide a conservative estimation even for a muscular model with 0% BFP, as is evident from (A2) since the intercept in (8) is smaller than unity. The limitation of this equation is that the number of models considered is at most 13 as listed in table 1, and so the uncertainty is estimated based on extrapolation, because muscular model is not available. Allowing for the compensation coefficient  $F$ , the coefficient determination was improved to 0.897 from 0.859 for (6) only. (A1) and (A2) provided reasonable WBA-SARs; the maximal and average differences were 18.2% and 7.1%, respectively, which are an improvement over the values presented in Sec. 3.4.

The WBA-SAR in free space was largely affected by BFP (Hirata *et al* 2010). One of the primary reasons was that the current takes its maximal value around the abdomen where tissue composition is affected by the BFP. On the other hand, the current takes its maximal value around the ankle for grounded humans. The coefficient of determination for the regression line using the compensation coefficient from (A1) was 0.896 for the grounded human models and

0.996 for eight models previously studied in free space (Hirata *et al* 2010). Thus, the estimation formula was not so improved, even if we allowed for BFP for grounded human models, unlike in free space.

## References

- Altman P L and Dittmer D S 1974 *Biology Data Book: Blood and Other Body Fluids*, Washington, DC: Federation of American Societies for Experimental Biology
- Conil E, Hadjem A, Lacroux F, Wong M F, and Wiart J 2008 Variability analysis of SAR from 20 MHz to 2.4 GHz for different adult and child models using finite-difference time-domain *Phys. Med. Biol.* **53** 1511-25
- Conil E, Hadjem A, Gati A, Wong M F, and Wiart J 2011 Influence of plane-wave incidence angle on whole body and local exposure at 2100 MHz *IEEE Trans. Electromagnet. Compat.* **53** 48-52
- Dimbylow P J 1997 FDTD calculations of the whole-body averaged SAR in an anatomically realistic voxel model of the human body from 1 MHz to 1 GHz *Phys. Med. Biol.* **42** 479-90
- Dimbylow P J 2002 Fine resolution calculations of SAR in the human body for frequencies up to 3 GHz *Phys. Med. Biol.* **47** 2835-46
- Dimbylow P J 2005 Resonance behavior of whole-body averaged specific energy absorption rate (SAR) in the female voxel model, NAOMI *Phys. Med. Biol.* **50** 4053-63
- Dimbylow P and Bolch W 2007 Whole-body-averaged SAR from 50 MHz to 4 GHz in the University of Florida child voxel phantoms *Phys. Med. Biol.* **52** 6639-49
- Dimbylow P J, Hirata A, and Nagaoka T 2008 Intercomparison of whole-body averaged SAR in European and Japanese voxel phantoms *Phys. Med. Biol.* **53** 5883-97
- Durney C H 1980 Electromagnetic dosimetry for models of humans and animals: a review of theoretical and numerical techniques *Proc. IEEE* **68** 33-40
- El Habachi A, Conil E, Hadjem A, Vazquez E, Wong M F, Gati A, Fleury G, and Wiart J 2010 Statistical analysis of whole-body absorption depending on anatomical human characteristics at a frequency of 2.1 GHz *Phys. Med. Biol.* **55** 1875-87
- Findlay R P and Dimbylow P J 2005 Effects of posture on FDTD calculations of specific absorption rate in a voxel model of the human body *Phys. Med. Biol.* **50** 3825-35
- Findlay R P and Dimbylow P J 2006 Variations in calculated SAR with distance to the perfectly matched layer boundary for a human voxel model *Phys. Med. Biol.* **51** N411-5
- Findlay R P and Dimbylow P J 2008 Calculated SAR distributions in a human voxel phantom due to the reflection of electromagnetic fields from a ground plane between 65 MHz and 2 GHz *Phys. Med. Biol.* **53** 2277-89
- Fujiwara O, Hirata A, Nagaoka T, and Watanabe S 2006 Dependence of whole-body average SAR on angle of incidence for plane-wave exposure *Record of 2006 Tokai-Section Joint Conf. of the Eight Inst. of Electr. Related Eng.* O-083
- Gabriel S, Lau R W, and Gabriel C 1996 The dielectric properties of biological tissues: III. Parametric models for the dielectric spectrum of tissues *Phys. Med. Biol.* **41** 2271-93

- Gandhi O P 1980 State of the knowledge for electromagnetic absorbed dose in man and animals  
*Proc. IEEE* **68** 24-32
- Kraus J D and Marhefka R J 2002 Antennas for all applications, 3rd Ed. McGraw-Hill, NY
- Komiyama S, Masuda T, Nakao T, and Teramoto K 2004 The relationships between stature, fat-free mass index, and fat mass index at before and after BMI-rebound in children *J. Health Sci.* **26** 31-9
- Lee A K and Choi H-D 2012 Determining the influence of Korean population variation on whole-body average SAR *Phys. Med. Biol.* **57** 2709-25
- Nagaoka T, Watanabe S, Sakurai K, Kunieda E, Watanabe S, Taki M, and Yamanaka Y 2004 Development of realistic high-resolution whole-body voxel models of Japanese adult males and females of average height and weight, and application of models to radio-frequency electromagnetic-field dosimetry *Phys. Med. Biol.* **49** 1-15
- Nagaoka T, Togashi T, Saito K, Takahashi M, Ito K, and Watanabe S 2007 An anatomically realistic whole-body pregnant-woman model and specific absorption rates for pregnant-woman exposure to electromagnetic plane waves from 10 MHz to 2 GHz **52** 6731-45
- Nagaoka T, Kunieda E, and Watanabe S 2008 Proportion-corrected scaled voxel models for Japanese children and their application to the numerical dosimetry of specific absorption rate for frequencies from 30 MHz to 3 GHz *Phys. Med. Biol.* **53** 6695-11
- Nagaoka T and Watanabe S 2008 Postured voxel-based human models for electromagnetic dosimetry *Phys. Med. Biol.* **53** 7047-61
- Hirata A, Caputa K, Dawson T W, and Stuchly M A 2001 Dosimetry in models of child and adult for low-frequency electric fields *IEEE Trans. Biomed. Eng.* **83** 1007-12.
- Hirata A, Kodera S, Wang J, and Fujiwara O 2007 Dominant factors influencing whole-body average SAR due to far-field exposure in whole-body resonance frequency and GHz regions *Bioelectromagnetics* **28** 484-7
- Hirata A, Fujiwara O, Nagaoka T, and Watanabe S 2010 Estimation of whole-body average SAR in human models due to plane-wave exposure at resonance frequency, *IEEE Trans. Electromagnet. Compat.* **52** 41-8
- International Commission on Non-Ionizing Radiation Protection (ICNIRP) 1998 Guidelines for limiting exposure to time-varying electric, magnetic, and electromagnetic fields (up to 300 GHz) *Health Phys.* **74** 494-522
- International Commission on Non-Ionizing Radiation Protection (ICNIRP) 2009 Statement on the “Guidelines for limiting exposure to time-varying electric, magnetic, and electromagnetic fields (up to 300 GHz)” *Health Phys.* **97** 257-8
- ICRP 1975 Report of the Task Group on Reference Man (Oxford, UK: International

- Commission on Radiological Protection Publication)
- Japanese Society of Nutritional Assessment 2001 Japanese Anthropometric Reference Data: Body Mass Index
- Japanese Society for Pediatric Endocrinology 2011 BMI data sheet  
[http://jspe.umin.jp/ipp\\_taikaku.htm](http://jspe.umin.jp/ipp_taikaku.htm)
- Kawamura Y, Hikage T, and Nojima T 2010 Experimental quasi-microwave whole-body averaged SAR estimation method using cylindrical-external field scanning *IEICE Trans. Comm.* **93** 1826-33
- Komiyama S, Masuda T, Nakao T, and Teramoto K 2004 The relationships between stature, fat-free mass index, and fat mass index at before and after BMI-rebound in children *J. Health Sci.* **26** 31-9
- Kühn S, Jennings W, Christ A, and Kuster N 2009 Assessment of induced radio-frequency electromagnetic fields in various anatomical human body models *Phys. Med. Biol.* **54** 875-90
- Lean M E, Han T S, and Deurenberg P 1996 Predicting body composition by densitometry from simple anthropometric measurements *Am. J. Clin. Nutrition*, **63** 4-14
- Laakso I, Ilvonen S, and Uusitupa T 2007 Performance of convolutional PML absorbing boundary conditions in finite-difference time-domain SAR calculations *Phys. Med. Biol.* **52** 7183-92
- Miyatake N, Takenami S, Kawasaki Y, Kunihashi Y, Nishikawa H, and Numata T 2005 Clinical evaluation of body fat percentage in 11,833 Japanese measured by air displacement plethysmograph *Internal Med.* **44** 702-5
- Penman A D and Johnson W D 2006 The changing shape of the body mass index distribution curve in the population: implications for public health policy to reduce the prevalence of adult obesity *Prev. Chronic Dis.* **3** A74
- Peyman A, Gabriel C, Grant E H, Vermeeren G, and Martens L 2009 Variation of the dielectric properties of tissues with age: the effect on the values of SAR in children when exposed to walkie-talkie devices *Phys. Med. Biol.*, **54** 227-42
- Pietrobelli A, Faith M S, Allison D B, Gallagher D, Chiumello G, and Heymsfield S B 1998 Body mass index as a measure of adiposity among children and adolescents: a validation study *J. Pediatr.* **132** 204-10
- Poljak D, Tham C Y, Gandhi O, and Sarolic A 2003 Human equivalent antenna model for transient electromagnetic radiation exposure," *IEEE Trans. Electromagn. Compat.* **45** 141-5
- Research Institute of Human Engineering for Quality Life 2006 Body size database of Children 2005-2006 (<http://www.hql.jp/database/index.html>)

- Sandrini L, Vaccari A, Malacarne C, Cristoforetti L, and Pontalti 2004 RF dosimetry: comparison between power absorption of female and male numerical models from 0.1 to 4 GHz *Phys. Med. Biol.* **49** 5185-201
- Uusitupa T, Laakso I, Ilvonen S, and Nikoskinen K 2010 SAR variation study from 300 to 5000 MHz for 15 voxel models including different postures *Phys. Med. Biol.* **55** 1157-76
- Taflove A and Hagness S 2003 *Computational Electrodynamics: The Finite-Difference Time-Domain Method*: 3rd Ed. Norwood, MA: Artech House
- Wang J, Fujiwara O, and Watanabe S 2006 Approximation of aging effect on dielectric tissue properties for SAR assessment of mobile telephones. *IEEE Trans. Electromagnet. Compat.*, **48** 408–13
- World Health Organization 2010 WHO RF Research Agenda  
[http://whqlibdoc.who.int/publications/2010/9789241599948\\_eng.pdf](http://whqlibdoc.who.int/publications/2010/9789241599948_eng.pdf)
- Zannolli R and Morgese G 1996 Distribution of BMI in children: prevalence of wasting and fattening conditions *Ann. Hum. Biol.* **23** 63-9

## Figure and Table Captions

Figure 1. Computational condition and exposure scenario.

Figure 2. WBA-SARs in TARO for different human-ground distances at the frequency of 39 MHz which is the resonance frequency for grounded TARO. WBA-SAR values are normalized by that in free space.

Figure 3. (a) Normalized WBA-SARs in the models of Japanese adult male and children for different human-ground distances. The WBA-SAR was normalized by that in free space. (b) Normalized resonance frequencies in the models of Japanese adult male and children for different human-ground distances normalized by respective model heights. The resonance frequencies were normalized by that in free space: 65 MHz, 97 MHz, and 136 MHz for the models of adult male, 7-year-old, and 3-year-old children.

Figure 4. The amplitude of vertical component of the conduction current in the Japanese body models of adult male and children at their respective resonance frequencies.

Figure 5. (a) Relationship between model's height and effective height for different human models, and (b) relationship between the square of induced voltage and absorbed power in the thirteen body models.

Figure 6. Effect of model inhomogeneity on the amplitude of vertical conduction current in the models of Japanese adult male and children at their respective resonance frequencies.

Figure 7. Comparison of WBA-SARs for homogeneous and inhomogeneous Japanese human body models.

Figure 8. Variability of estimated WBA-SARs by Equation (6) for the inhomogeneous model with BMI of 2.5–97.5%ile. The incident power density is  $2 \text{ W m}^{-2}$ . As a conservative estimate, the estimated WBA-SAR for the homogeneous model with BMI of 2.5%ile is also plotted.

Table 1. Height, weight, BMI, and number of tissue types for human models considered in this study.

Table 2. Total average power [W] absorbed in the mother and fetus of grounded Japanese pregnant women model computed by researchers from three institutes. The incident power density is  $2 \text{ W m}^{-2}$  at 46 MHz.

Table 3. Comparison of FDTD-calculated, estimated WBA-SARs by Equation (6) ( $\times 10^{-2} \text{ W/kg}$ ), the corresponding difference on WBA-SARs, and resonance frequency in different human body models. The incident power density is  $2 \text{ W m}^{-2}$ .

Figure A1. Effect of body fat percentage on the WBA-SAR normalized by that for a homogeneous model with an electrical constant equal to  $2/3$  that of muscle. The curve for  $\alpha\%$  muscle was calculated for a homogenized Japanese male adult model TARO.

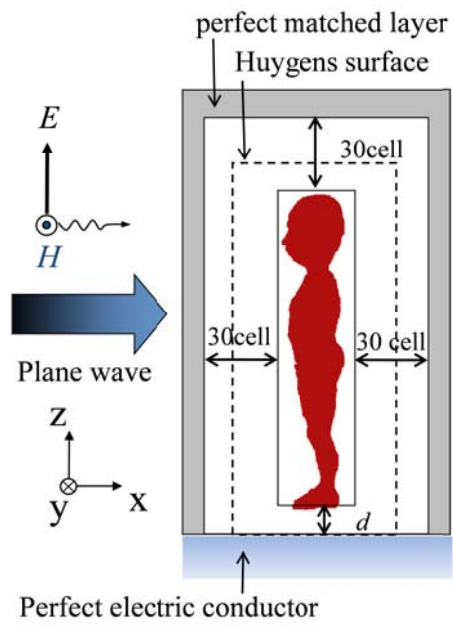


Fig. 1

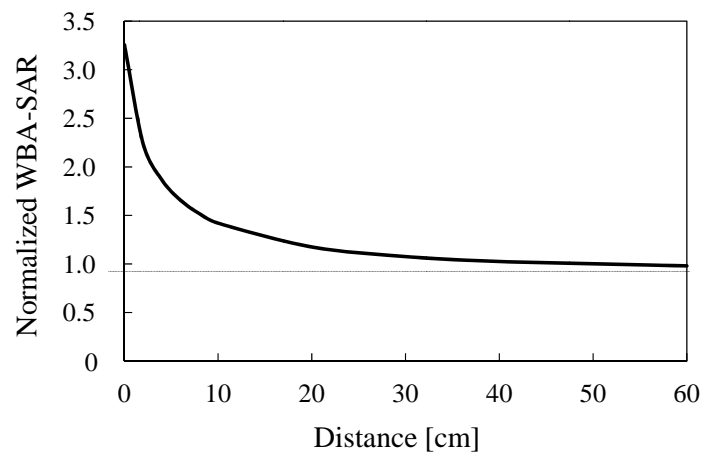
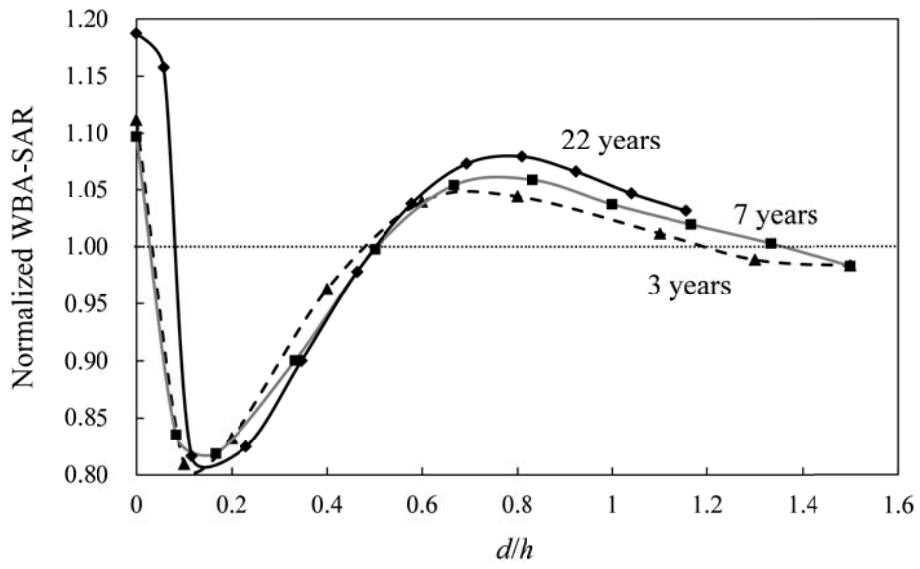
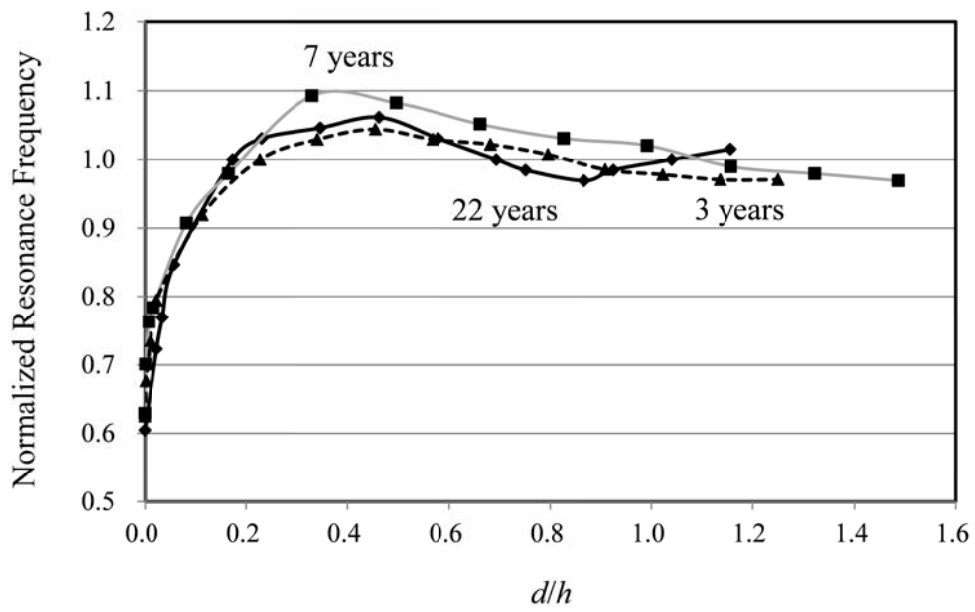


Fig. 2



(a)



(b)

Fig. 3

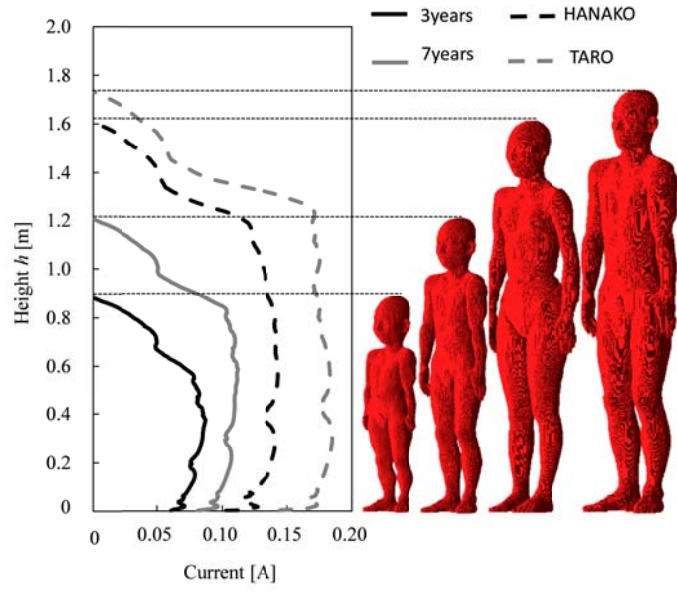
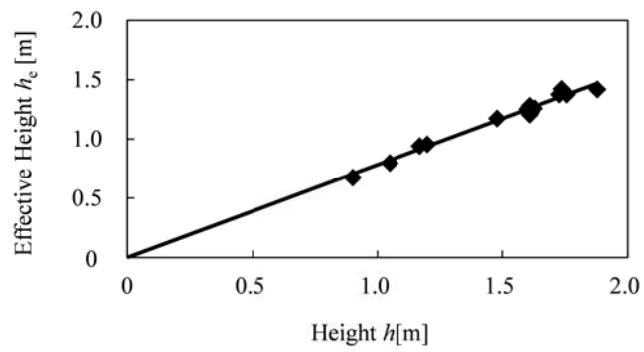


Fig. 4



(a)

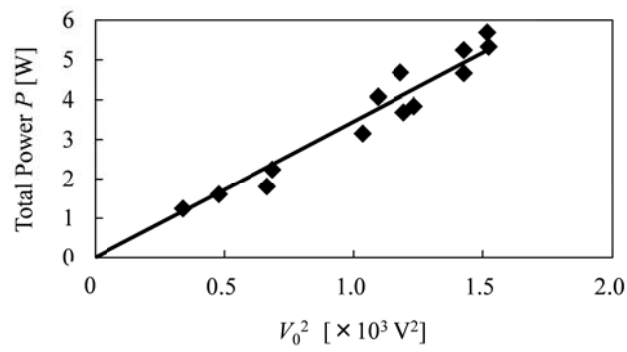


Fig. 5 (b)

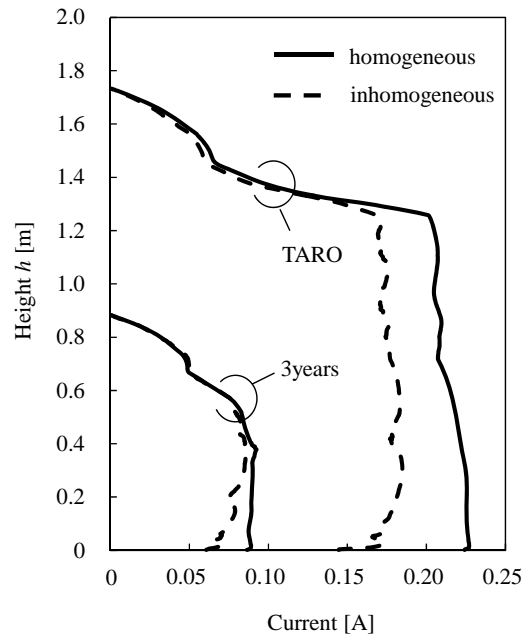


Fig. 6

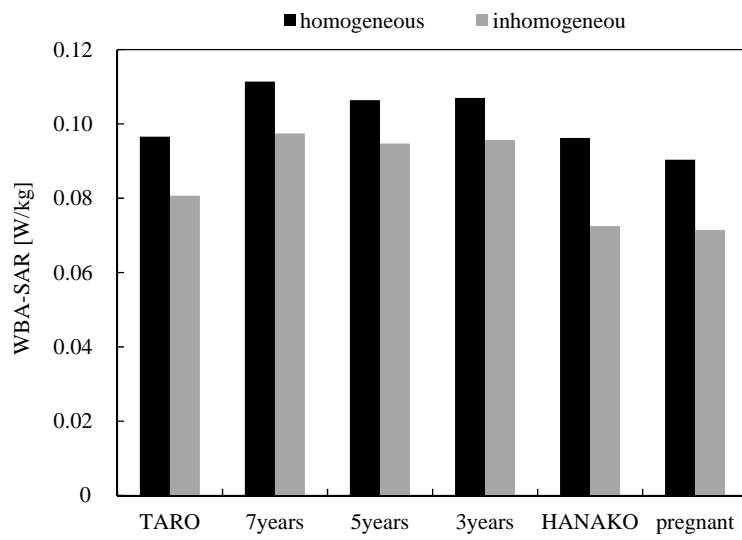


Fig. 7

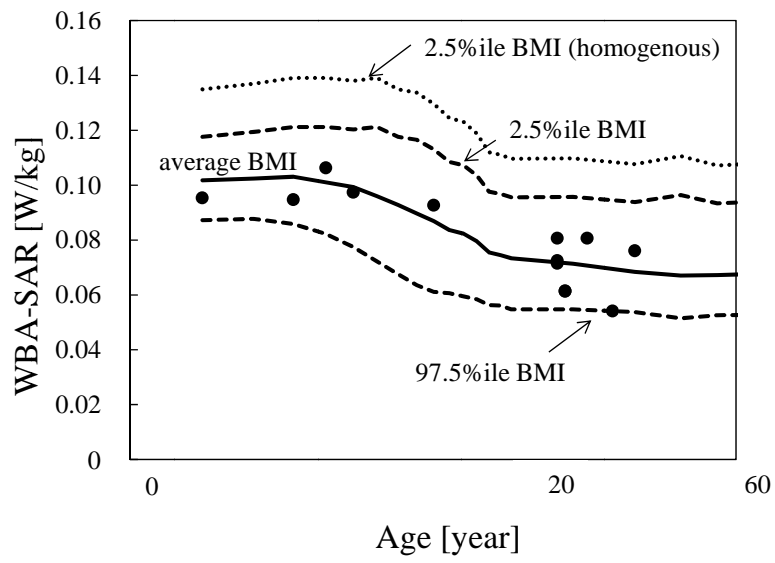


Fig. 8

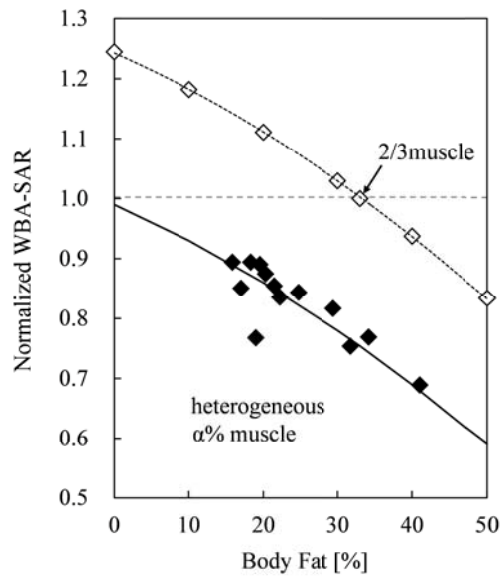


Fig. A1

Table 1

Models	TARO	7years	5years	3years	HANAKO	PregnantWoman
Height [m]	1.73	1.20	1.05	0.90	1.61	1.61
Weight [kg]	65	23	17	13	53	58
BMI [ $\text{kg m}^{-2}$ ]	21.7	16.0	15.4	16.0	20.4	22.4
Number of Tissues	51	51	51	51	51	56

Models	Duke	Ella	Billie	Thelonious	NORMAN	NAOMI	BAFB
Height [m]	1.74	1.60	1.48	1.17	1.76	1.63	1.88
Weight [kg]	70	58	34	17	76	60	105
BMI [ $\text{kg m}^{-2}$ ]	23.1	22.7	15.5	12.4	24.5	22.6	29.7
Number of tissues	84	84	84	84	37	41	39

Table 2

	NIT	Orange Lab.	NICT
Mother	5.08	5.14	5.21
Fetus	0.0115	0.0112	0.0109

Table 3

	TARO	7years	5years	3years	HANAKO	PregnantWoman	
FDTD-calculated WBA-SAR [ $\times 10^{-2}$ W/kg]	8.07	9.74	9.47	9.54	7.25	7.15	
Estimated WBA-SAR by Equation (6) [ $\times 10^{-2}$ W/kg]	7.33	9.97	10.33	9.93	7.79	7.23	
Diff. [%]	-9.3	2.1	8.9	3.5	7.2	1.2	
Resonance frequency [MHz]	39	61	73	85	45	46	

	BAFB	NORMAN	NAOMI	Duke	Ella	Billie	Thelonious
FDTD-calculated WBA-SAR [ $\times 10^{-2}$ W/kg]	5.41	6.13	6.15	7.61	8.07	9.27	10.63
Estimated WBA-SAR by Equation (6) [ $\times 10^{-2}$ W/kg]	5.35	6.48	7.04	6.88	7.02	10.24	12.80
Diff. [%]	-1.2	5.6	14.5	-9.6	-13.2	10.5	20.43
Resonance frequency [MHz]	38	40	48	40	42	51	66